RESEARCH ARTICLE

Enhanced Na^+-K^+-$2Cl^-$ Cotransporter 1 Underlies Motor Dysfunction in Huntington's Disease

Yi-Ting Hsu, MD,[1,2] Ya-Gin Chang, BS,[3,4] Yu-Chao Liu, PhD,[3] Kai-Yi Wang, BS,[3] Hui-Mei Chen, BS,[5] Ding-Jin Lee, BS,[1] Sung-Sen Yang, MD, PhD,[6] Chon-Haw Tsai, MD, PhD,[1,2] Cheng-Chang Lien, MD, PhD[3,7]* and Yijuang Chern, PhD[1,3,5]*

[1]*PhD Program for Translational Medicine, China Medical University and Academia Sinica, Taipei, Taiwan*
[2]*Department of Neurology, China Medical University Hospital, Taichung, Taiwan*
[3]*Institute of Neuroscience, National Yang-Ming University, Taipei, Taiwan*
[4]*Taiwan International Graduate Program in Interdisciplinary Neuroscience, National Yang-Ming University and Academia Sinica, Taipei, Taiwan*
[5]*Institute of Biomedical Sciences, Academia Sinica, Taipei, Taiwan*
[6]*Division of Nephrology, Department of Medicine, Tri-Service General Hospital, National Defense Medical Center, Taipei, Taiwan*
[7]*Brain Research Center, National Yang-Ming University, Taipei, Taiwan*

ABSTRACT: Background: Altered γ-*aminobutyric acid* signaling is believed to disrupt the excitation/inhibition balance in the striatum, which may account for the motor symptoms of Huntington's disease. Na-K-2Cl cotransporter-1 is a key molecule that controls γ-*aminobutyric acid*-ergic signaling. However, the role of Na-K-2Cl cotransporter-1 and efficacy of γ-*aminobutyric acid*-ergic transmission remain unknown in Huntington's disease.

Methods: We determined the levels of Na-K-2Cl cotransporter-1 in brain tissue from Huntington's disease mice and patients by real-time quantitative polymerase chain reaction, western blot, and immunocytochemistry. Gramicidin-perforated patch-clamp recordings were used to measure the $E_{\gamma\text{-}aminobutyric\ acid}$ in striatal brain slices. To inhibit Na-K-2Cl cotransporter-1 activity, R6/2 mice were treated with an intraperitoneal injection of bumetanide or adeno-associated virus-mediated delivery of Na-K-2Cl cotransporter-1 short-hairpin RNA into the striatum. Motor behavior assays were employed.

Results: Expression of Na-K-2Cl cotransporter-1 was elevated in the striatum of R6/2 and $Hdh^{150Q/7Q}$ mouse models. An increase in Na-K-2Cl cotransporter-1 transcripts was also found in the caudate nucleus of Huntington's disease patients. Accordingly, a depolarizing shift of $E_{\gamma\text{-}aminobutyric\ acid}$ was detected in the striatum of R6/2 mice. Expression of the mutant *huntingtin* in astrocytes and neuroinflammation were necessary for enhanced expression of Na-K-2Cl cotransporter-1 in HD mice. Notably, pharmacological or genetic inhibition of Na-K-2Cl cotransporter-1 rescued the motor deficits of R6/2 mice.

Conclusions: Our findings demonstrate that aberrant γ-*aminobutyric acid*-ergic signaling and enhanced Na-K-2Cl cotransporter-1 contribute to the pathogenesis of Huntington's disease and identify a new therapeutic target for the potential rescue of motor dysfunction in patients with Huntington's disease. © 2019 International Parkinson and Movement Disorder Society

Key Words: bmetanide; GABAergic signaling; inflammation; mutant Huntingtin; NKCC1

***Correspondence to:** Yijuang Chern, Institute of Biomedical Sciences, Academia Sinica, Nankang, Taipei 115, Taiwan; E-mail: bmychern@ibms.sinica.edu.tw; or Dr. Cheng-Chang Lien, Institute of Neuroscience, National Yang-Ming University, Taipei 112, Taiwan; E-mail: cclien@ym.edu.tw

Ya-Gin Chang and Yu-Chao Liu contributed equally to this article.

Relevant conflicts of interest/financial disclosures: All authors report no financial relationships with commercial interests.

Funding agencies: This work was supported by grants from the Ministry of Science and Technology (NSC101-2321-B-001-047, MOST 104-2811-B-001-123, to Y.C.; MOST 106-2320-B-010-011-MY3 to C.C.L.; MOST 104-2314-B-039-031-MY2, to Y.T.H.), China Medical University Hospital (CRS-106-060), Academia Sinica (AS-100-TP2-B02), Taiwan, and the Brain Research Center, National Yang-Ming University from the Featured Areas Research Center Program (to C.C.L) within the framework of the Higher Education Sprout Project by the Ministry of Education (MOE) in Taiwan.

Received: 10 December 2018; **Revised:** 29 January 2019; **Accepted:** 4 February 2019

Published online 00 Month 2019 in Wiley Online Library (wileyonlinelibrary.com). DOI: 10.1002/mds.27651

Huntington's disease (HD) is an autosomal-dominant neurodegenerative disease characterized by its clinical manifestations of cognitive deficits, involuntary movements, and psychiatric symptoms. Expanded CAG repeats in exon 1 of the *huntingtin* (*htt*) gene cause neuronal cell death, occurring most severely in the striatum of HD brains.[1] Despite the extensive studies devoted to the characterization of HD pathogenesis and the development of effective therapies, little is currently available for the treatment of HD patients.

The balance between the excitatory glutamatergic system and the inhibitory γ-*aminobutyric acid* (GABA)-ergic system within the corticostriatal circuitry is critical for normal control of motor function, cognition, and behavior.[2] Dysfunction of either the glutamatergic system or the GABAergic system has been implicated in a spectrum of neuropsychiatric disorders, such as schizophrenia, autism spectrum disorder, Parkinson's disease, major depressive disorder, and HD.[3] Conversely, modulation of the GABAergic system has potential implications in the treatment of several neuropsychiatric disorders.[4,5] GABA, the major inhibitory neurotransmitter in the adult brain, exerts its action via synaptic and extrasynaptic $GABA_A$ receptors ($GABA_A$Rs) to mediate phasic and tonic inhibition, respectively.[4,6] The hyperpolarizing inhibitory action of the $GABA_A$ receptor depends on the proper maintenance of the transmembrane chloride gradient, which is mainly controlled by 2 cation-chloride cotransporters: Na-K-2Cl cotransporter (NKCC1) and K-Cl cotransporter (KCC2).[7] NKCC1 mediates chloride uptake in immature neurons and causes high intracellular chloride levels and a depolarizing GABA response. As neurons mature, KCC2 becomes the principal chloride cotransporter that extrudes chloride out of the cell and switches the excitatory nature of GABAergic transmission to inhibitory.[7] Previous studies have found that the GABAergic system in HD brains is disrupted.[8-10] Nonetheless, the pathogenic nature of GABAergic dysregulation and the roles of Cl^- dysregulation in the HD striatum during disease progression remain largely uncharacterized.

Astrocytes regulate multiple aspects of neuronal and synaptic function through several mechanisms.[11] In several HD mouse models, detrimental astrocytic activities have been demonstrated to impair neuronal functions through cell and non-cell autonomous effects.[12-14] For example, dysregulation of the astrocytic Kir4.1 channel aggravates neuronal excitability in HD by disturbing the astrocyte-mediated potassium homeostasis.[12] Inflammation caused by abnormal glial activation also significantly contributes to neuronal damage in HD.[13,15] Poor potassium buffering in astrocytes may contribute to the overactivation of neuronal NKCC1,[16] and proinflammatory cytokines may regulate the expression of NKCC1.[17,18] Here, we hypothesized that the expression of NKCC1 might be altered in the inflammatory environment in HD brains, and we aimed to investigate whether the polarity of GABAergic signaling was altered and contributed to HD pathogenesis. To test this hypothesis, we first determined the expression and function of NKCC1 in different HD mouse models and postmortem human caudate nuclei by biochemical and/or electrophysiological methods. We further modulated the NKCC1-regulated GABAergic signaling in HD mice by pharmacological and genetic inhibition of NKCC1 and assessed the HD phenotypes.

Materials and Methods

More detailed information on materials and methods is provided in SI Materials and Methods section.

Animals and Treatments

Three transgenic mouse models (R6/2 [B6CBA-Tg (HDexon1)62Gpb/1J], N171-82Q [B6C3F1/J- Tg (HD82Gln)81Dbo/J], GFAP-HD [FVB/N-Tg(GFAP-HTT*160Q)-31Xjl/J]) and 1 knock-in HD mouse model ($Hdh^{150Q/7Q}$ [B6.129P2-Hdhtm2Detl/J]) were originally obtained from the Jackson Laboratory (Bar Harbor, ME). Transgenic R6/2 mice contain exon 1 of the human *htt* gene harboring an expansion of the CAG repeat (181 ± 4).[19] The N171-82Q mice express a cDNA fragment encoding an N-terminal fragment of Huntingtin (HTT) with 82 glutamines driven by the mouse prion protein promoter.[20] GFAP-HD mice express CAG-expanded HTT in glial cells under the control of the human glial fibrillary acidic protein (GFAP) promoter.[14] $Hdh^{150Q/7Q}$-knock-in mice express the endogenous *htt* gene harboring 150 CAG repeats.[21] Mice were genotyped by polymerase chain reaction (PCR)[13] and were housed at the Institute of Biomedical Sciences Animal Care Facility (Taipei, Taiwan) under a 12-hour light/dark cycle. All behavioral experiments were performed during the light phase. To avoid the potential subtle differences in the course of neurodegeneration, we chose to do all experiments, except for Figure S1, using female mice. To confirm that the upregulation of NKCC1 in the brain of HD mice is sex independent, we tested the male HD mice (R6/2, 10 weeks old) and found that upregulation of NKCC1 also occurred in the striata of male HD mice. All animal experiments were performed in accordance with protocols approved by the Academia Sinica Institutional Animal Care and Utilization Committee (Taipei, Taiwan).

For intracerebroventricular (icv) delivery of XPro1595 (a generous gift from Xencor, Monrovia, CA), R6/2 and their littermate control (wild-type) mice were treated with XPro1595 (0.08 mg/kg/day) or saline using osmotic minipumps (micro-osmotic pump 1004, brain infusion kit 3; Alzet, Cupertino, CA) into the lateral ventricle from the age of 6.5 to 10.5 weeks, as described elsewhere.[22]

For systemic treatment with bumetanide, R6/2 mice and their littermate control mice were randomly assigned to the bumetanide group (0.2 mg/kg of body

weight in 0.3% dimethylsulfoxide [DMSO]; Sigma, St. Louis, MO) and the vehicle group (0.3% DMSO in saline) and treated daily for 6 weeks by intraperitoneal injection from the age of 7 weeks

For the in vivo delivery of adeno-associated viral vectors (AAVs) carrying short-hairpin RNA (shRNA) knockdown of *NKCC1*, R6/2 mice and their littermate control mice at age 5 weeks were intrastriatally injected with the indicated AAV, as described elsewhere[13] and detailed in the SI Methods section.

Human Brain Samples

Postmortem human brain tissue of the caudate nucleus was obtained from 2 sources. Brain sections of the caudate nucleus were obtained from the National Institute of Child Health and Human Development Brain and Tissue Bank for Developmental Disorders (University of Maryland, Baltimore, MD) and analyzed by immunofluorescence staining. RNA from the caudate nucleus for quantitative PCR (qPCR) was obtained from the Human Brain and Spinal Fluid Resource Center (VA West Los Angeles Healthcare Center, Los Angels, CA). The demographic data and neuropathology of subjects are summarized in Table S1.

RNA Purification and Real-Time qPCR

RNA was isolated from mouse brains and human postmortem tissue and converted to cDNA using methods previously described.[23] mRNA level was determined by quantitative PCR. The ΔΔCt method was used to determine the relative fold expression of mRNA,[24] which was then normalized to that of the wild-type group. Glyceraldehyde-3-phosphate dehydrogenase (*GAPDH)* and 18S ribosomal RNA were used as the reference genes for the mouse and human postmortem brain samples, respectively.

Western Blot Analysis

Protein samples were collected from cells or dissected brain regions of the mouse with lysis buffer, separated by 4%-10% sodium dodecyl sulfate polyacrylamide gel electrophoresis and then transferred to polyvinylidene fluoride (PVDF) membranes. The PVDF membranes were blocked and incubated overnight at 4°C with primary antibodies followed by peroxidase-conjugated secondary antibodies. Protein expression was calculated by normalizing the protein signal to that of valosin-containing protein (VCP) or tubulin as the loading control.

Immunohistochemical Staining

Sections from the human caudate nucleus or mouse striatum were subjected to immunohistochemistry as previously described.[13] The sections were incubated with the indicated primary antibody followed by incubation with the corresponding secondary antibody. Fluorescent images were acquired using an LSM780 confocal microscope with ZEN software. For the detection of polyQ-expanded HTT, coronal sections (20 μm) of mouse striatum were subjected to immunohistochemistry with an anti-HTT antibody (EM48; Millipore Corporation, Billerica, MA) and a Vectastain ABC immunoperoxidase kit (Vector) with 3,3-diaminobenzidine (DAB) (Sigma-Aldrich) as a chromogen. Three pictures spaced evenly throughout the striatum were taken using a CCD camera (Axio Imager Z1 Microscope, Zeiss), and 9 pictures from 3 sections for each animal were analyzed. The immunostaining patterns and quantification of NKCC1 and mutant Huntingtin (mHTT) expression were analyzed with the aid of MetaMorph software (Universal Imaging, West Chester, PA).

Slice Preparation and Perforated-Patch Recording

To avoid perturbation of the intracellular chloride concentration, we evaluated the GABA reversal potential (E_{GABA}) of medium spiny neurons (MSNs) using the gramicidin-perforated patch-clamp recordings,[25] detailed in the SI Methods. Notably, monitoring membrane leakage is critical during the measurement of E_{GABA}.[26-28] The integrity of the perforated patch configuration was assessed in cells by adding Alexa Fluor 594 to the pipette solution. To monitor the stability of the recording, we recorded epifluorescence images of the same cell before and after measurement of the E_{GABA}. No correction for liquid junction potentials was made. Only experiments with the fluorescent dye Alexa Fluor 594, restricted to the recording pipette, were considered to ensure the integrity of the perforated patch.

Behavioral Assessment

Mice were tested for limb-clasping behavior by holding the mice from the tail and suspending them for 30 seconds. The degree of limb clasping was scored using the following rules: 0, no clasping; 1, clasping by either the fore- or hind limbs; and 2, clasping by both the fore- and hind limbs. Motor coordination was monitored using a rotarod apparatus assay (Ugo Basile, Comerio, Italy), as described elsewhere.[13] Briefly, mice were tested at a constant speed of 12 rpm over a period of 2 minutes. Each mouse was tested 3 times per week, and each test contained 3 trials for a maximum of 2 minutes for each trial. The time of the latency to fall was automatically recorded.

Statistical Analysis

Data are represented as the mean ± SEM. All tests were performed using SigmaStat (version 3.5, Systat Software, Richmond, CA). The Student *t* test (2-tailed, 95% confidence interval) or the Mann-Whitney test was used to compare the difference between the 2 groups. One-way or 2-way analysis of variance (ANOVA) was

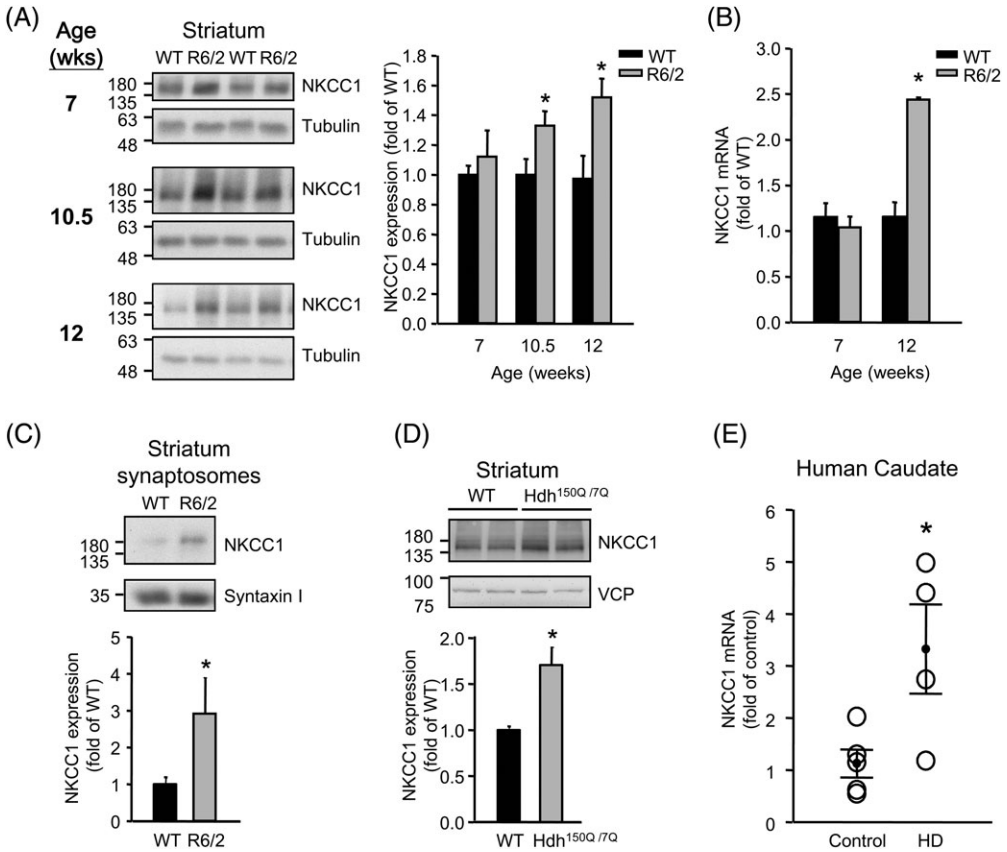

FIG. 1. NKCC1 expression is increased in the striatum of HD. (A) Representative immunoblots for NKCC1 in total protein extracts from the striatum of R6/2 mice and littermate controls (wild type) at different ages. The quantification of NKCC1 expression was performed relative to that of α-tubulin (n = 6). (B) *NKCC1* mRNA level was assessed by quantitative reverse-transcription PCR (RT-qPCR) and normalized to the expression of a reference gene (*GAPDH*) in the striatum of wild-type (n = 6) and R6/2 (n = 6) mice. (C) Representative immunoblots for NKCC1 in synaptosomal fractions from the striatum of wild-type and R6/2 mice at 12 weeks of age. The quantification of NKCC1 expression compared with that in wild-type mice was performed relative to that of syntaxin I (n = 4). (D) Representative immunoblots for NKCC1 in total protein extracts from the striatum of wild-type and $Hdh^{150Q/7Q}$ mice at 17 months of age. The quantification of NKCC1 expression was performed relative to that of VCP (n = 3). All data are presented as the mean ± SEM. *$P < 0.05$ compared with the wild type by the Student *t* test. (E) Frozen human postmortem caudate tissues (n = 5 for the non-HD group and n = 4 for the HD group) were used for RNA preparation and the following RT-qPCR analysis. The reference gene was *18S rRNA*. All data are presented as the mean ± SEM. *$P < 0.05$ compared with non-HD subjects by the Student *t* test.

used when the differences among multiple groups were compared, followed by the appropriate post hoc tests, as indicated in the figure legends. A $P < 0.05$ was defined as significant.

Results

NKCC1 Expression Is Increased in the Striatum of HD

To characterize the role of NKCC1 in HD pathogenesis, we first examined NKCC1 level in a transgenic mouse model of HD (R6/2).[19] NKCC1 protein level in the striata of R6/2 mice at the manifest stage (10.5 weeks old) was higher than that of wild-type mice (Figs. 1A and S1). The extent of the increase in NKCC1 protein became more evident when the disease progressed to the final stage in R6/2 mice. A marked increase in the transcript level of *NKCC1* was also observed in the striata of R6/2 mice (Fig. 1B), suggesting that the enhanced expression of NKCC1 may occur at the transcriptional level. Of note, expression of NKCC1 was also upregulated in the cortex, a brain area that is also greatly affected by HD,[29] but not in the hippocampus of R6/2 mice (Fig. S2). We further found the increased NKCC1 protein in the synaptosomal fractions prepared from the HD striatum was much more significant than in the unfractionated lysates (Fig. 1C). We suggest that the upregulation of NKCC1 in the brains of R6/2 mice might predominantly occur in neurons.

We next evaluated whether NKCC1 level was also enhanced in $Hdh^{150Q/7Q}$ mice, a knock-in mouse model.[21] Western blot analysis showed that the amount of NKCC1 protein in the striata of $Hdh^{150Q/7Q}$ mice was also higher than in wild-type mice (Fig. 1D). To determine whether the aberrantly elevated levels of the NKCC1 protein observed in HD mice were an authentic pathogenesis of HD, we performed experiments to determine whether this abnormality could be found in HD postmortem brains. NKCC1 level in the caudates of HD patients was assessed by double immunofluorescence staining of NKCC1 and

NeuN. A trend toward an increase in NKCC1 was found in neurons (ie, NeuN-positive cells) of HD patients (n = 3, Table S1) when compared with those from non-HD subjects (n = 4, $P = 0.053$; Fig. S3). We also determined the transcript levels of *NKCC1* in the postmortem caudates of 4 HD patients and 5 non-HD subjects (Table S1). Reverse-transcription polymerse chain reaction (RT-PCR) analyses showed that HD patients exhibited more *NKCC1* transcripts than did non-HD subjects in the caudate (Fig. 1E).

Striatal Neurons of R6/2 Mice Exhibit a Positive Shift in E_{GABA}

A previous study showed that upregulation of NKCC1 in neurons results in elevated intracellular [Cl^-] and a shift of E_{GABA} toward more depolarized potentials.[30] To assess whether the enhanced expression of NKCC1 resulted in chloride dysregulation in HD striatal neurons, we directly measured the reversal potential for $GABA_A$R-mediated Cl^- currents (E_{GABA}) of MSNs in striatal brain slices prepared from wild-type and HD (R6/2) mice using the gramicidin-perforated patch-clamp technique.[25] With the fluorescent dye Alexa Fluor 594 in the patch pipettes, the integrity of the cell membrane was confirmed by epifluorescence illumination (Fig. 2A). The measurement of $GABA_A$R-mediated Cl^- currents was conducted by holding the MSNs at different membrane potentials in the voltage clamp (Fig. 2B). The value of E_{GABA} from each MSN was obtained from a polynomial fit (Fig. 2B). The E_{GABA} recorded from the MSNs of wild-type mice was not correlated with the mouse age ($r^2 = 0.002$), whereas the E_{GABA} recorded from R6/2 mice showed a positive correlation with mouse age ($r^2 = 0.466$); see Figure 2C. The average E_{GABA} from R6/2 MSNs after the manifest stage was significantly more depolarized than the E_{GABA} of wild-type MSNs (Fig. 2D). To evaluate whether the positive shift of the E_{GABA} was because of enhanced NKCC1, we further determined the E_{GABA} of neurons treated with a NKCC1 inhibitor, bumetanide. Bumetanide significantly changed the E_{GABA} in neurons from R6/2 mice but not in those of wild-type (WT) mice at the manifest stage (Fig. 2D). Notably, the resting membrane potential

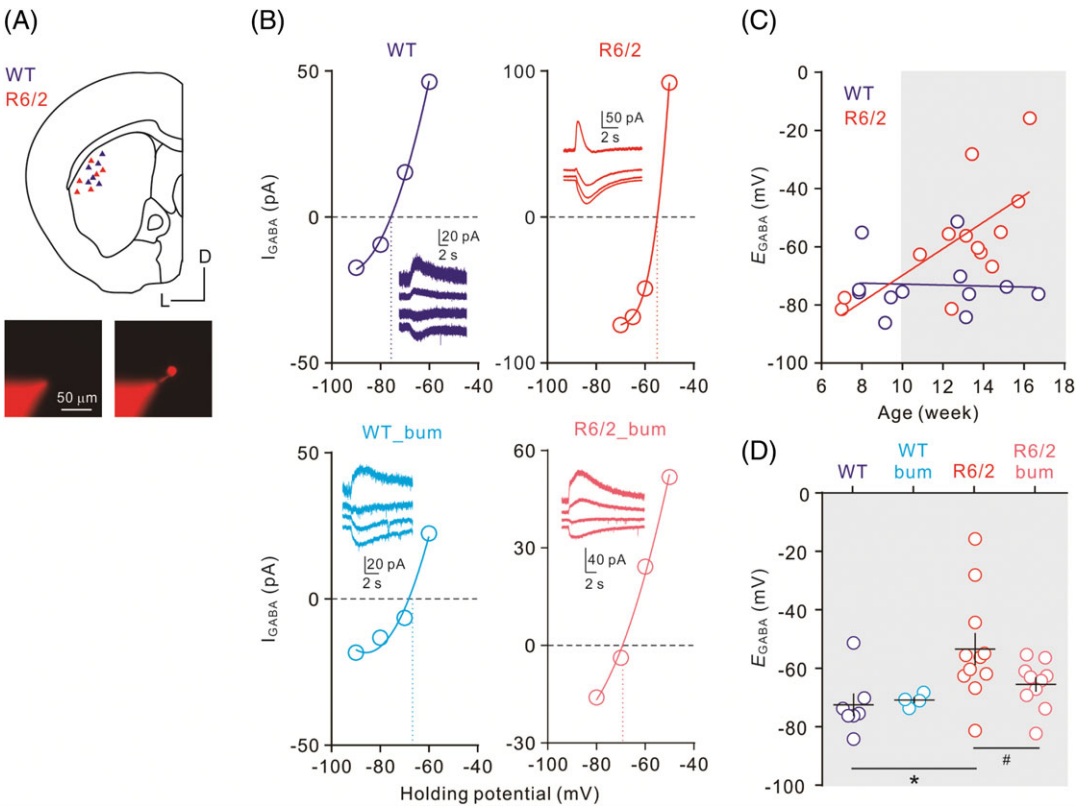

FIG. 2. Striatal medium spiny neurons (MSNs) exhibit a less negative E_{GABA} in R6/2 mice than in wild-type mice. (A) Gramicidin-perforated recording of dorsolateral MSNs from wild-type and R6/2 mice was made from the premanifest to the late manifest stages. The integrity of the cell membrane was confirmed by epifluorescence illumination. (B) Examples of the current-voltage relationship of GABA currents (I_{GABA}) elicited by puffing muscimol (a selective $GABA_A$R agonist; 20 μM) to the neuronal cell body. The vertical dotted lines indicate the value of E_{GABA} on the *x* axis. Insets show sample traces of muscimol-induced currents at different holding potentials. (C) The E_{GABA} recorded from MSNs of wild-type mice was not correlated with mouse age ($r^2 = 0.002$), whereas, the E_{GABA} recorded from R6/2 mice showed a positive correlation with mouse age ($r^2 = 0.466$). The gray area denotes the manifest stage. (D) Summary of E_{GABA} with and without bumetanide (bum, 10 μM) bath application from wild-type and R6/2 MSNs at the manifest stage. Average E_{GABA} from R6/2 MSNs at the manifest stage was significantly more depolarized than the E_{GABA} of neurons from wild-type mice. Wild type, -72.5 ± 3.9 mV, n = 7; R6/2, -53.5 ± 5.5 mV, n = 11; wild-type_bum, -70.9 ± 1.1 mV, n = 4; R6/2_bum, -65.5 ± 2.6 mV, n = 10. *Comparison between wild-type and R6/2, $p = 0.02$; #comparison between R6/2 and R6/2_bum, $P = 0.04$; Mann-Whitney test. WT, wild type.

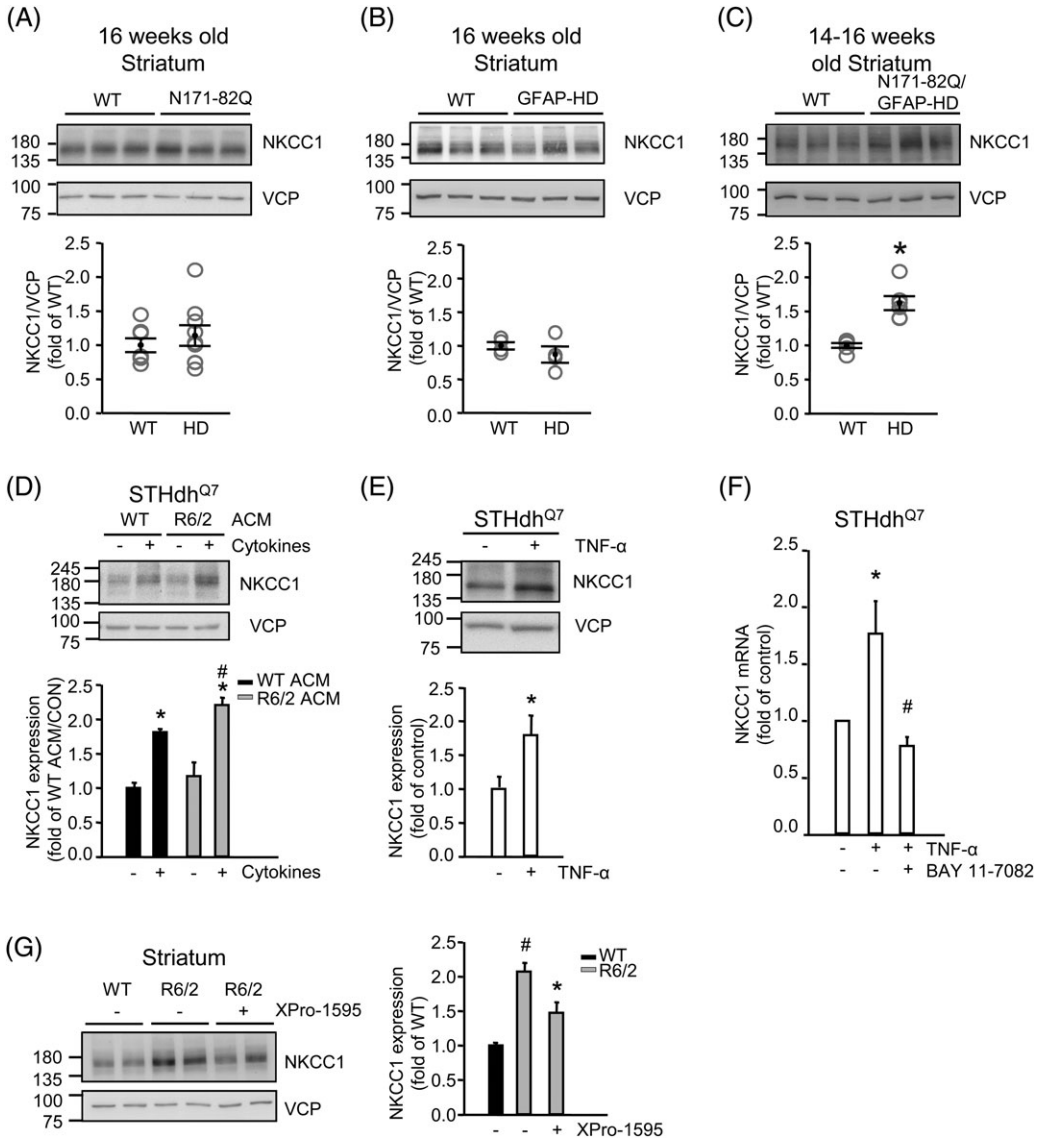

FIG. 3. Neuroinflammation contributes to the increased NKCC1 in HD mice. (A-C) Expression of NKCC1 was determined by western blot analysis. The striatum of the indicated HD mice at the manifest stage (for A, N171-82Q, n = 7-9, 16 weeks of age; for C, double transgenic N171-82Q/GFAP-HD mice, n = 6, 14-16 weeks of age) or the premanifest stage (for B, GFAP-HTT-160Q, n = 4, 16 weeks of age) was carefully removed for protein preparation. The quantification of NKCC1 expression was performed relative to that of VCP. The data are presented as the mean ± SEM. *$P < 0.05$ compared with wild-type mice by the Student *t* test. (D) ST*Hdh*^{Q7} cells were treated with astrocyte-conditioned medium (ACM) collected from wild-type (WT) or R6/2 astrocytes stimulated with or without cytokines (10 ng/mL TNF-α and 10 ng/mL IL-1β) for 2 days. NKCC1 level in total lysate was determined by western blot analysis and normalized to VCP. The data are presented as the mean ± SEM of 3 independent experiments. *Specific comparison between vehicle- and cytokine-treated cells of the same group; #specific comparison between wild-type and R6/2 ACM with the same treatment; $P < 0.05$ by 1-way ANOVA. (E) ST*Hdh*^{Q7} cells were directly treated with 20 ng/mL TNF-α for 6 hours. Expression of NKCC1 was assessed by western blot and normalized to VCP. The data are presented as the mean ± SEM of 3 independent experiments. *$P < 0.05$ compared with vehicle-treated cells by the Student *t* test. (F) TNF-α stimulation (20 ng/mL, 6 hours) of the ST*Hdh*^{Q7} cells resulted in increased transcript levels of *NKCC1*, which was reversed by pretreatment with BAY 11-7082 (5 μM, 1 hour). The transcript levels were measured by quantitative reverse transcription PCR (RT-qPCR) and normalized to the expression of a reference gene (*GAPDH*). The data are presented as the mean ± SEM of 3 independent experiments. *$P < 0.05$ compared with vehicle-treated cells; #$P < 0.05$ compared with cytokine-treated cells by 1-way ANOVA. (G) Infusion of XPro1595 into the brain by a minipump decreased the level of NKCC1 in R6/2 mice. Mice were given an icv infusion of XPro1595 or saline as control by an osmotic minipump, which delivered 0.08 mg/kg/day XPro1595 or saline, at 6.5-10.5 weeks old. Striatal tissues were collected 4 weeks after the initial injection. The expression levels of NKCC1 in the striatum were determined by western blot analysis. The results were normalized to the expression levels of VCP. The data are presented as the mean ± SEM (n = 5-8 mice per group). *Specific comparison between vehicle- and XPro1595-treated mice of the same group; #specific comparison between wild-type and R6/2 mice with the same treatment; $P < 0.05$ by Tukey's post hoc test following 1-way ANOVA. WT, wild type.

(V_m) of MSNs in the wild-type and R6/2 mice did not significantly differ (wild type, -70 ± 8 mV, n = 7; R6/2, -72 ± 6 mV, n = 9; $P = 0.83$). Consistent with previous results, elevated NKCC1 led to a progressive increase in the E_{GABA} in the MSNs of R6/2 mice during disease progression.

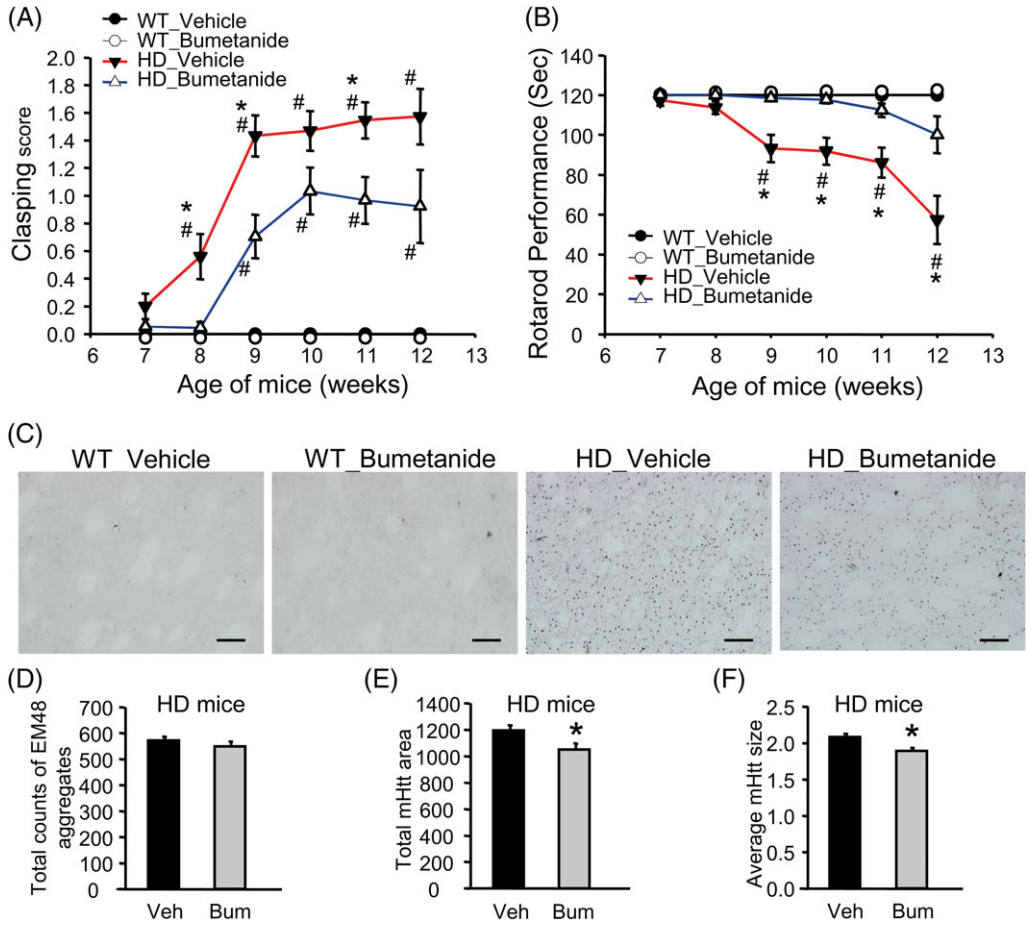

FIG. 4. Pharmacological inhibition of NKCC1 improves motor performance and reduces the size of mHTT aggregates in R6/2 mice. R6/2 and wild-type mice were treated daily for 6 weeks with bumetanide (0.2 mg/kg of body weight intraperitoneally) or vehicle (0.3% DMSO in saline) from 7 weeks of age. Limb clasping (A) and rotarod performance (B) were measured weekly between ages 7 and 12 weeks. The data are presented as the mean ± SEM (n = 10-11 animals per group). *Specific comparison between vehicle- and bumetanide-treated mice of the same group; #specific comparison between wild-type and R6/2 mice with the same treatment; $P < 0.05$ by Tukey's post hoc test following 2-way ANOVA. The results are representative of 2 independent experiments. Because bumetanide treatment did not affect either clasping or rotarod behaviors of WT mice, the symbol of solid circles (control group) is masked by the open circles (treated group). WT, wild type; HD, Huntington's disease. (C) Brain sections were collected after chronic bumetanide (0.2 mg/kg/day) therapy for 6 weeks and were immunohistochemically stained to detect mHTT with an anti-HTT antibody (EM48). Representative mHTT aggregate staining in the striatum of WT and R6/2 mice. EM48-positive mHTT aggregates were detected in the R6/2 striatum and were absent in the WT striatum. Bumetanide treatment reduced the size of the mHTT aggregates. Scale bars, 50 μm. (D-F) Quantification of the total counts, area, and average size of the mHTT aggregates. Bars represent total count, total area or average size of the mHTT aggregates ± SEM (n = 6 animals per group). *Specific comparison between vehicle- and bumetanide-treated (0.2 mg/kg/day) mice of the same group; $P < 0.05$ by the Student *t* test. [Color figure can be viewed at wileyonlinelibrary.com]

Neuroinflammation Contributes to the Abnormal Upregulation of NKCC1 in HD Brains

Although aberrant upregulation of NKCC1 was observed in neurons, western blot analysis showed that there was no change in the NKCC1 level in the striatum of a mouse model (N171-82Q), which expressed mHTT only in neurons,[20] at the end stage of disease (16 weeks old, Fig. 3A). Conversely, GFAP-HD mice, which expressed mHTT only in astrocytes,[14] had more NKCC1 protein in the striata than did wild-type mice at the manifest stage (18-24 months old; Fig. S4,), but not before the onset of motor deficits (16 weeks old; Fig. 3B). Most importantly, significant NKCC1 upregulation was observed in the striata of mice (14-16 weeks old) that expressed mHTT in both neurons and astrocytes (designated N171-82Q/GFAP-HD mice; Fig. 3C). These data collectively suggest that mHTT-dysregulated astrocytes may have mediated NKCC1 upregulation in neurons and that the simultaneous expression of mHTT in neurons greatly sensitized this process.

Previous studies have demonstrated that expression of mHTT in astrocytes leads to alterations in multiple astrocytic properties.[12,13,31] We were particularly interested in the potential involvement of proinflammatory cytokines in the NKCC1 upregulation observed in HD brains because of the recently recognized association between inflammation and cation chloride cotransporters.[17,18] To evaluate the effect of astrocytic inflammation on neuronal NKCC1 expression, we first prepared astrocyte-conditioned medium (ACM) that was harvested from

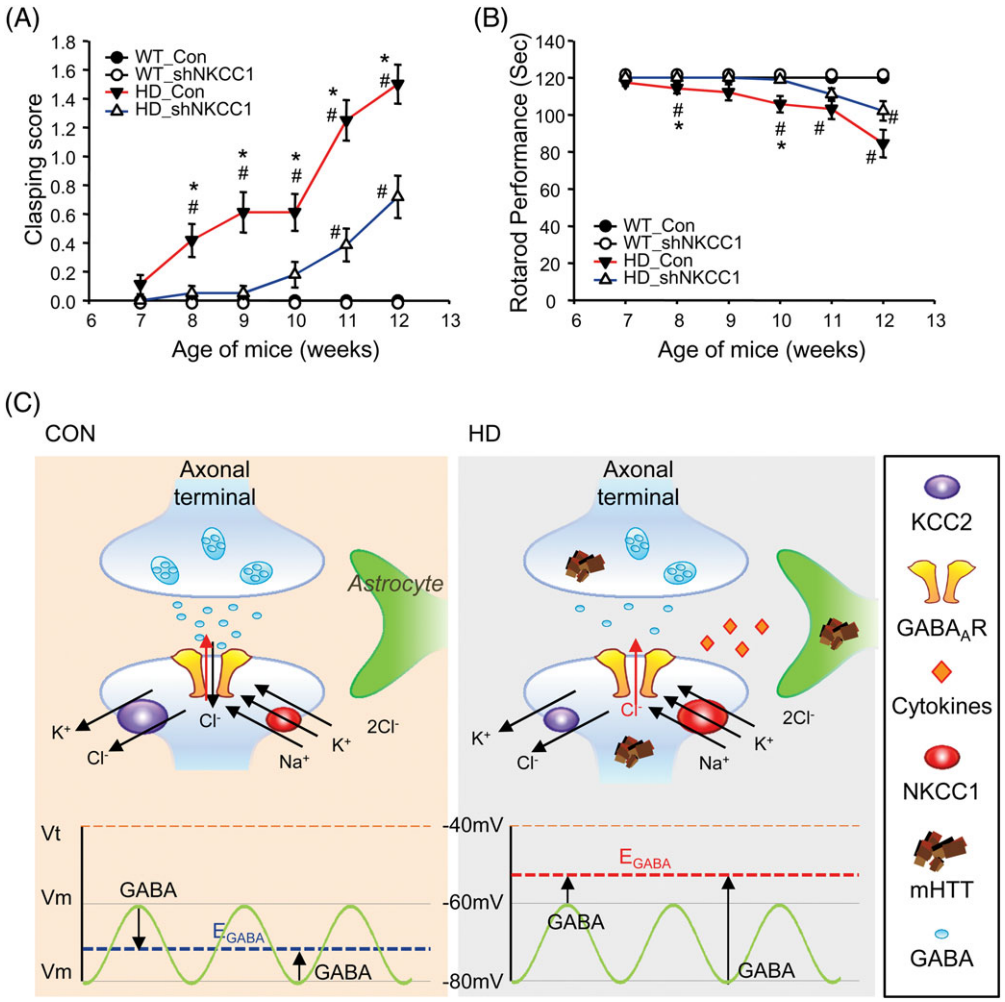

FIG. 5. Genetic reduction of NKCC1 delays the motor impairment in R6/2 mice. Mice (5 weeks of age) received a viral injection of AAV carrying an shRNA of NKCC1 or an irrelevant control protein into the striatum. (A, B) Limb clasping and rotarod performance were measured weekly between ages 7 and 12 weeks. The data are presented as the mean ± SEM (n = 12-14 animals per group). *Specific comparison between AAV-Con-infected mice and shRNA of NKCC1-infected mice of the same group; #specific comparison between wild-type and R6/2 mice with the same treatment; $P < 0.05$ by Tukey's post hoc test following 2-way ANOVA. The results are representative of 2 independent experiments. Because injection of AAV carrying shNKCC1 did not affect either clasping or rotarod behaviors of WT mice, the symbol of solid circles (control group) is masked by the open circles (treated group). WT, wild type; HD, Huntington's disease. (C) A schematic representation showing the proposed mechanism of elevated NKCC1 and the positive shift of E_{GABA} in HD neurons. In HD neurons, elevated NKCC1 caused by proinflammatory cytokines leads to high intracellular Cl^- and a positive shift of E_{GABA}. The E_{GABA} in HD neurons could be greater than or equal to the V_m during the down and up states, resulting in depolarizing or shunting inhibitory response. The depicted membrane potentials mimicked the in vivo membrane potential fluctuations. $GABA_AR$, $GABA_A$ receptor; HD, Huntington's disease; KCC2, K-Cl cotransporter; mHTT, mutant huntingtin; NKCC1, Na-K-2Cl cotransporter; V_m, membrane potential; V_t, threshold for action potentials.

primary wild-type and R6/2 cortical/striatal astrocytes (30 *days in vitro*) that were treated with cytokines for 72 hours. The effect of these ACMs on the expression of NKCC1 in a striatal progenitor cell line (STHdh^{Q7}) was determined by western blot analysis. As shown in Figure 3D, STHdh^{Q7} cells expressed higher levels of NKCC1 protein when treated with ACM collected from astrocytes that were activated with cytokines than from astrocytes without cytokine activation. Notably, ACM collected from R6/2 astrocytes treated with cytokines evoked greater elevation in NKCC1 than did ACM collected from wild-type astrocytes treated with cytokines, which may be ascribed to the higher release of inflammatory mediators by R6/2 astrocytes than by wild-type astrocytes during stimulation with cytokines.[13]

To consolidate the role of cytokines in NKCC1 upregulation, we treated STHdh^{Q7} cells with a well-characterized proinflammatory cytokine (tumor necrosis factor α [TNF-α]). Treatment with TNF-α was sufficient to increase the protein and transcript levels of NKCC1 in STHdh^{Q7} cells (Fig. 3E,F). Given that treatment with TNF-α could activate the nuclear factor kappa-light-chain-enhancer of activated B cells (NF-κB) pathway,[32] we hypothesized that activated NF-κB might regulate *NKCC1* transcription. To test this hypothesis, STHdh^{Q7} cells were treated with TNF-α in the presence of an NF-κB inhibitor (BAY 11-7082).

RT-qPCR revealed that BAY11-7082 effectively reduced the NF-κB-evoked *NKCC1* upregulation (Fig. 3F), confirming the importance of NF-κB signaling.

To validate that neuroinflammation plays a critical role in NKCC1 upregulation in vivo, we infused a dominant-negative inhibitor of soluble TNF-α (XPro1595)[33] into the brains of HD mice (R6/2) using a protocol that has been shown to reduce the production of proinflammatory cytokines in the brains of R6/2 mice and to reduce their motor dysfunction.[22] We found that chronic treatment with XPro1595 in the brain markedly reduced NKCC1 protein level in the striatum (Fig. 3G). Collectively, these findings suggest that neuroinflammation may mediate the enhanced NKCC1 expression in HD brains.

Inhibition of NKCC1 Ameliorates the Motor Phenotype in HD Mice (R6/2)

To evaluate whether NKCC1 upregulation contributes to HD progression, we inhibited the function of NKCC1 using bumetanide[30] and assessed disease progression by measuring motor function, body weight, and life span. R6/2 mice received bumetanide (0.2 mg/kg of body weight, daily intraperitoneal injection) starting from the presymptomatic stage (7 weeks old). Administration of bumetanide significantly attenuated motor impairment in R6/2 mice, assessed by the rotarod performance and foot-clasping tests (Fig. 4A,B). The beneficial effects were detected as early as in weeks 8-9, in which the elevation of NKCC1 protein was not yet at peak levels (shown to occur near 12 weeks; Fig. 1A). This suggests that NKCC1 protein function is inhibited by bumetanide. Previous studies have demonstrated that phosphorylation of NKCC1 at threonine residues activates NKCC1, leading to the active uptake of chloride.[34] Our data show that a higher level of phosphorylated NKCC1 was found in the striata of R6/2 mice when compared with WT mice. Treatment with bumetanide significantly decreased the phosphorylation of NKCC1 in the striata of R6/2 mice at age 9 weeks, when the beneficial effect was observed (Fig. S5). Thus, bumetanide may prevent NKCC1 activation via modulating phosphorylation and subsequently rescue the impaired motor function in HD mice.

When compared with those treated with vehicle, chronic treatment with bumetanide also slightly decreased the size of the mHTT aggregates by approximately 10% without affecting the number of mHTT aggregates (Fig. 4C-F). Nonetheless, no improvement in reduced body weight, shortened life span, reduced expression of *DARPP32*, or increased expression of *NKCC1* by bumetanide was observed (Figs. S6 and S7). In addition, no significant effect of bumetanide on the level of proinflammatory cytokines was observed either (Fig. S8), suggesting that there was no significant loop impact of a NKCC1 inhibitor on the development of the neuroinflammatory pathway in the HD striatum.

Suppression of NKCC1 in the brains of R6/2 mice was also conducted by direct injection of AAV harboring shRNA against *NKCC1* (ie, shNKCC1) into the striata of R6/2 mice at age 5 weeks. The efficiency of AAV-mediated knockdown of *NKCC1* was assessed in vitro and in vivo. Exogenous expression of shNKCC1 reduced the amount of NKCC1 protein in N2A cells by approximately 50% (Fig. S9A). We also examined the expression of *NKCC1* transcript in the striata of mice infected with viruses carrying shNKCC1 or the control virus (ie, shCon). As shown in Figure S9B, HD mice (R6/2) infected with the control virus had higher *NKCC1* than did WT mice, as predicted. Infection of R6/2 mice with viruses harboring shNKCC1 reduced the amount of *NKCC1* transcripts to a level indistinguishable from that of WT mice. Improvements in motor function were observed with the genetic suppression of NKCC1 in the striata of R6/2 mice (Fig. 5A,B). Taken together, our data suggest that upregulation of NKCC1 during HD progression contributes to the motor impairment observed in HD.

Discussion

Progressive motor dysfunction is a major functional disability of HD and is often the reason for nursing home placement.[35,36] Tetrabenazine and its modified form (deutetrabenazine), which reduce the amount of dopamine in the brain, are the only 2 drugs approved by the Food and Drug Administration for the treatment of motor dysfunction in HD. Adverse effects such as depression and suicidal behaviors can limit the clinical use of tetrabenazine and possibly deutetrabenazine as well.[37] There is clearly an unmet need for drugs available to patients with HD. To date, the pathophysiological role of GABAergic signaling in motor control during HD progression has attracted only limited attention. Earlier studies have reported several GABAergic abnormalities in HD brains caused by altered $GABA_AR$-mediated synaptic currents, disruption of $GABA_AR$ trafficking, and reduced expression of $GABA_AR$.[8-10] Nonetheless, the aberrant polarity and poor efficacy of GABAergic signaling in the striatum during HD progression have not been extensively characterized. The coordinated activities of NKCC1 and KCC2 control neuronal chloride homeostasis and are responsible for the polarity of GABAergic signaling.[7] We detected enhanced expression of NKCC1 in the cortices and striata but not in the hippocampi of R6/2 mice, whereas Dargaei et al[38] found increased NKCC1 expression in both the cortices and hippocampi of R6/2 mice. The factors that contribute to this seemingly discrepant finding are currently unknown. First, the R6/2 mice used in the present study and those of Dargaei et al[38] differed in their CAG repeat number (181 ± 4 and 120 ± 5 CAG repeats, respectively), age (12 and 7 weeks, respectively), and sex (female only and both sexes, respectively). Next,

R6/2 mice are susceptible to the development of seizures,[39] which was reported to induce high levels of hippocampal NKCC1[40] and might be subjected to different procedures of mouse handling in different animal facilities. Some of these factors might contribute to the discrepancy in the hippocampal NKCC1 level in R6/2 mice.

Decreased expression of KCC2 has been previously reported when increased NKCC1 was observed and may enable GABA to become excitatory.[41] Likewise, our group[23] and Dargaei et al[38] reported reduced KCC2 expression in the cortices, striata, and hippocampi of multiple HD mouse models. Consistently, we and Dargaei et al[38] reported that the stronger depolarization of E_{GABA} was mainly because of the increased expression of NKCC1 in R6/2 mice rather than the reduced expression of KCC2, because acute application of an NKCC1 inhibitor, bumetanide, restored normal E_{GABA} values. Notably, NKCC1 inhibition by bumetanide rescued the memory deficits[38] and motor phenotype of R6/2 mice. Moreover, we found that genetic downregulation of striatal NKCC1 rescued the motor defect in R6/2 mice, indicating the importance of NKCC1 in HD pathogenesis. These findings suggest that the efficacious $GABA_AR$-mediated inhibitory signaling in HD brains may become less effective.

An intriguing finding from the present study is that the expression of mHTT in astrocytes alone was sufficient to trigger NKCC1 upregulation (GFAP-HD mice) and that expression of mHTT in neurons greatly facilitated the NKCC1 upregulation triggered by mHTT-expressing astrocytes (N171-82Q/GFAP-HD mice). The results from both in vitro and in vivo experiments suggest that proinflammatory cytokines released from astrocytes during inflammation in the final stage of HD in mice are likely to trigger NKCC1 upregulation in neurons at the transcriptional level. Our findings are consistent with several earlier studies that have reported that production of proinflammatory cytokines was able to upregulate NKCC1 expression on vascular endothelium, lung epithelial cells, and astrocytes.[17,42,43] Nonetheless, the mechanism by which inflammatory cytokines (eg, TNF-α) regulate the expression of NKCC1 remains elusive. Interestingly, an earlier study showed that proinflammatory mediators (such as TNF-α) may alter gene profiles by activating NF-κB-dependent transcription.[32] Bioinformatics analysis using the PROSCAN[44] and PROMO programs[45] predicted that there are NF-κB-binding sites in mouse and human *NKCC1* promoters. In addition, previous studies have shown that inhibition of NF-κB may reduce the activity or protein expression of NKCC1.[46,47] The involvement of NF-κB in the regulation of NKCC1 expression in response to inflammation and/or mutant HTT-evoked stresses is of interest and requires further investigation. In the present study, we found that an inhibitor of NF-κB (BAY 11-7082) significantly blocked the TNF-α-induced upregulation of the *NKCC1* transcript, demonstrating that NF-κB activation might increase the transcriptional levels of *NKCC1*. Khoshnan and colleagues have previously reported that expression of mHTT enhances the NF-κB pathway by direct binding to and activation of the IKKβ complex, which results in activation of NF-κB and aggravation of mHTT-evoked toxicity in neurons.[48] In astrocytes, mHTT enhances NF-κB-mediated inflammatory responses that greatly contribute to HD pathogenesis.[13] Inflammation is an important detrimental element in HD, as blockage of TNF-α using XPro1595 in vivo leads to significant beneficial effects on disease progression in HD mice.[22] Our findings suggest that the aberrant activation of NF-κB-mediated inflammation may alter neuronal function via upregulation of NKCC1 in neurons and impair neuronal responses to GABAergic stimuli. Because neurons expressing mHTT exhibit abnormally enhanced NF-κB activity,[48] NF-κB-mediated actions (such as NKCC1 upregulation) in response to proinflammatory cytokines are likely to be sensitized. This effect may explain the observation that HD astrocyte-mediated NKCC1 upregulation was greatly facilitated when there was also mutant HTT in neurons. In addition to astrocyte-mediated neuroinflammation, microglia have long been recognized as an important source of neuroinflammation in HD pathogenesis.[13,49] The relative contributions of astrocytes and microglia to neuroinflammation and neuronal NKCC1 regulation remain unknown. The complex interplay between these cells in HD pathogenesis also needs further investigation.

To acutely monitor E_{GABA}, we performed gramicidin-perforated patch-clamp recordings[25] to avoid perturbation of the intracellular chloride concentration. To ensure there was no membrane leakage, we measured the series resistance and membrane integrity of the perforated patch during the entire recording. In our study, resting membrane potential (-70 ± 8 mV, $n = 7$) was very close to the E_{GABA} in wild-type striatum (-72.5 ± 3.9 mV, $n = 7$). GABA may exert shunting inhibition under this condition or slightly hyperpolarizing inhibition if MSNs are in the up state or a depolarized stage. It is worth noting that intracellular recording studies in anesthetized rodents showed that MSNs display periodic shifts between the down state (ie, a hyperpolarized membrane potential stage with a membrane potential of approximately -80 mV) and the up state (ie, a depolarized stage with a membrane potential of approximately -60 mV).[50,51] Thus, the hyperpolarizing inhibition (ie, E_{GABA} < resting membrane potential) in vivo during the up state can be important.[50,51] Indeed, we observed a bimodal distribution of membrane potentials in the present study. Given that the spike threshold in MSNs is approximately -40 mV,[52,53] both regimes (ie, shunting inhibition, resting membrane potential < E_{GABA} < spike threshold; hyperpolarizing inhibition) may coexist under wild-type

striatum, and GABAergic synapses can exert inhibitory actions on MSNs. In the HD striatum, the resting membrane potential (-72 ± 6 mV, n = 9) was less than the E_{GABA} (-53.5 ± 5.5 mV, n = 11). Under this condition, the E_{GABA} could be greater than or equal to the resting membrane potential during the down- and up state, resulting in a depolarizing or shunting inhibitory response (Fig. 5C). Such an alteration is expected to greatly affect the functions of MSNs, which integrate glutamatergic inputs from the cortex and project GABAergic signals to neurons downstream of the basal ganglia nuclei. The inhibitory stimuli from GABAergic interneurons and the lateral inhibitory connections with neighboring MSNs form a collateral network of local inhibition.[54] The altered $GABA_AR$ signaling in MSNs might affect the local excitability of MSNs and change the overall output of striatum. Of note, the slicing procedure by itself might alter Cl^- gradients during slice preparations.[55] Such an effect might be compounded in neurons from R6/2 mice, which are more susceptible to inflammation than WT neurons. In addition, R6/2 mice are prone to epileptic seizures, which themselves might alter Cl^- reversal potentials.[40] Collectively, we cannot rule out the contribution of both factors (ie, the slicing procedure and epileptic seizures) to the positive shift in striatal E_{GABA} of R6/2 mice.

The upregulation of NKCC1 in adult brains has been known to convert neuronal responses to GABA, from a hyperpolarizing to a depolarizing response.[30,38] Such a GABA-mediated depolarizing signal may elevate intracellular $[Ca^{2+}]$, enhance expression of the pan-neurotrophin receptor $p75^{NTR}$, and cause neuronal death. Importantly, treatment with bumetanide is able to ameliorate the toxicity induced by NKCC1 upregulation.[56] Consistent with the hypothesis that NKCC1/$p75^{NTR}$ is critical for neuronal survival, blockage of $p75^{NTR}$ is associated with beneficial effects on corticostriatal synaptic function in HD mice.[57] Previous studies have also reported that blockade of NKCC1 reduces glutamate-induced neurotoxicity, decreases the accumulated ubiquitin-conjugated protein aggregates, and improves proteasome function in ischemic neurons.[58,59] This is important because clearance of mHTT is primarily mediated by the ubiquitin-proteasomal system, which is impaired in HD.[60] In HD mice (R6/2), we found that chronic treatment with bumetanide slightly decreased the size of mHTT aggregates, which may be ascribed to the improved proteasome activity with NKCC1 inhibition, as was found in ischemic neurons.[58,59] Total mHTT count was likely not affected by bumetanide because mHTT aggregates appear in the brain of R6/2 mice at the age of 4 weeks, whereas the treatment with bumetanide did not start until 7 weeks of age. Thus, earlier administration of bumetanide may have more significant effects on the mHTT aggregates of HD mice.

Phosphorylation mechanisms play an important role in the regulation of NKCC1. The WNK/SPAK kinase complex, composed of WNK (with no lysine) and SPAK (SPS1-related proline/alanine-rich kinase), effectively phosphorylates and activates NKCC1, whereas protein phosphatases (such as PP1 and PP2A) dephosphorylate NKCC1 and decrease the activity of NKCC1.[61] Earlier studies showed that **bumetanide treatment inhibited the activity and phosphorylation level of NKCC1 in cancer cells**[62] **and** dorsal root ganglia neurons,[63] **respectively, which is consistent with our data**. It is unclear whether bumetanide inhibits NKCC1 activity directly or indirectly via the modulation of upstream kinases and/or protein phosphatases in HD.

Alterations in the level of NKCC1 and the depolarizing GABA action have been linked to a number of neuropsychiatric disorders.[64] Inhibition of NKCC1 has been proposed to serve as a potential treatment for autism, schizophrenia, and seizure in clinical trials and case reports.[65-68] These reports argue for a critical role of aberrant GABAergic signaling in neurological and psychiatric disorders. In the current study, our findings suggest that the upregulation of NKCC1 and the positive shift of the E_{GABA} were pathogenic in HD because pharmacological inhibition or genetic ablation of NKCC1 restored the motor deficits of HD mice. Our data show, for the first time, that aberrantly increased striatal NKCC1 may serve as a causal link for the motor deficits in HD. Our findings advance the current knowledge of GABAergic signaling in HD pathogenesis and provide a new therapeutic approach toward HD via modulating the function of NKCC1. Notably, in addition to being able to treat the motor dysfunction of HD, bumetanide has also been shown to restore hippocampal synaptic plasticity and memory in a mouse model of Down syndrome.[30] Given that neuroinflammation has been implicated in most neurodegenerative diseases (including Parkinson's disease and Alzheimer's disease[15]), upregulation of NKCC1 may also play a critical role in other neurodegenerative diseases. ■

Acknowledgments: We thank David E. Szymkowski and Xencor (Monrovia, CA) for providing XPro1595. No author reports financial relationships with commercial interests.

References

1. Ross CA, Tabrizi SJ. Huntington's disease: from molecular pathogenesis to clinical treatment. Lancet Neurol 2011;10(1):83-98.
2. Graybiel AM, Aosaki T, Flaherty AW, Kimura M. The basal ganglia and adaptive motor control. Science 1994;265(5180):1826-1831.
3. Shepherd GM. Corticostriatal connectivity and its role in disease. Nat Rev Neurosci 2013;14(4):278-291.
4. Brickley SG, Mody I. Extrasynaptic GABA(A) receptors: their function in the CNS and implications for disease. Neuron 2012;73(1):23-34.
5. Rudolph U, Knoflach F. Beyond classical benzodiazepines: novel therapeutic potential of GABAA receptor subtypes. Nat Rev Drug Discov 2011;10(9):685-697.

6. Farrant M, Nusser Z. Variations on an inhibitory theme: phasic and tonic activation of GABA(A) receptors. Nat Rev Neurosci 2005;6 (3):215-229.
7. Kaila K, Price TJ, Payne JA, Puskarjov M, Voipio J. Cation-chloride cotransporters in neuronal development, plasticity and disease. Nat Rev Neurosci 2014;15(10):637-654.
8. Cepeda C, Galvan L, Holley SM, et al. Multiple sources of striatal inhibition are differentially affected in Huntington's disease mouse models. J Neurosci 2013;33(17):7393-7406.
9. Yuen EY, Wei J, Zhong P, Yan Z. Disrupted GABAAR trafficking and synaptic inhibition in a mouse model of Huntington's disease. Neurobiol Dis 2012;46(2):497-502.
10. Allen KL, Waldvogel HJ, Glass M, Faull RL. Cannabinoid (CB(1)), GABA(A) and GABA(B) receptor subunit changes in the globus pallidus in Huntington's disease. J Chem Neuroanat 2009;37(4): 266-281.
11. Allen NJ. Astrocyte regulation of synaptic behavior. Annu Rev Cell Dev Biol 2014;30:439-463.
12. Tong X, Ao Y, Faas GC, et al. Astrocyte Kir4.1 ion channel deficits contribute to neuronal dysfunction in Huntington's disease model mice. Nat Neurosci 2014;17(5):694-703.
13. Hsiao HY, Chen YC, Chen HM, Tu PH, Chern Y. A critical role of astrocyte-mediated nuclear factor-kappaB-dependent inflammation in Huntington's disease. Hum Mol Genet 2013;22(9):1826-1842.
14. Bradford J, Shin JY, Roberts M, Wang CE, Li XJ, Li S. Expression of mutant huntingtin in mouse brain astrocytes causes age-dependent neurological symptoms. Proc Natl Acad Sci U S A 2009; 106(52):22480-22485.
15. Wyss-Coray T, Mucke L. Inflammation in neurodegenerative disease--a double-edged sword. Neuron 2002;35(3):419-432.
16. Rangroo Thrane V, Thrane AS, Wang F, et al. Ammonia triggers neuronal disinhibition and seizures by impairing astrocyte potassium buffering. Nat Med 2013;19(12):1643-1648.
17. Huang LQ, Zhu GF, Deng YY, et al. Hypertonic saline alleviates cerebral edema by inhibiting microglia-derived TNF-α and IL-1β-induced Na-K-Cl cotransporter up-regulation. J Neuroinflammation 2014;11:102.
18. Morales-Aza BM, Chillingworth NL, Payne JA, Donaldson LF. Inflammation alters cation chloride cotransporter expression in sensory neurons. Neurobiol Dis 2004;17(1):62-69.
19. Mangiarini L, Sathasivam K, Seller M, et al. Exon 1 of the HD gene with an expanded CAG repeat is sufficient to cause a progressive neurological phenotype in transgenic mice. Cell 1996;87(3): 493-506.
20. Schilling G, Becher MW, Sharp AH, et al. Intranuclear inclusions and neuritic aggregates in transgenic mice expressing a mutant N-terminal fragment of huntingtin. Hum Mol Genet 1999;8(3): 397-407.
21. Lin CH, Tallaksen-Greene S, Chien WM, et al. Neurological abnormalities in a knock-in mouse model of Huntington's disease. Hum Mol Genet 2001;10(2):137-144.
22. Hsiao HY, Chiu FL, Chen CM, et al. Inhibition of soluble tumor necrosis factor is therapeutic in Huntington's disease. Hum Mol Genet 2014;23(16):4328-4344.
23. Hsu YT, Chang YG, Chang CP, et al. Altered behavioral responses to gamma-aminobutyric acid pharmacological agents in a mouse model of Huntington's disease. Mov Disord 2017;32(11):1600-1609.
24. Schmittgen TD, Zakrajsek BA, Mills AG, Gorn V, Singer MJ, Reed MW. Quantitative reverse transcription-polymerase chain reaction to study mRNA decay: comparison of endpoint and real-time methods. Anal Biochem 2000;285(2):194-204.
25. Ebihara S, Shirato K, Harata N, Akaike N. Gramicidin-perforated patch recording: GABA response in mammalian neurones with intact intracellular chloride. J Physiol 1995;484(Pt 1):77-86.
26. Vida I, Bartos M, Jonas P. Shunting inhibition improves robustness of gamma oscillations in hippocampal interneuron networks by homogenizing firing rates. Neuron 2006;49(1):107-117.
27. Heigele S, Sultan S, Toni N, Bischofberger J. Bidirectional GABAergic control of action potential firing in newborn hippocampal granule cells. Nat Neurosci 2016;19(2):263-270.
28. Schmidt T, Ghaffarian N, Philippot C, et al. Differential regulation of chloride homeostasis and GABAergic transmission in the thalamus. Sci Rep 2018;8(1):13929.
29. de la Monte SM, Vonsattel JP, Richardson EP, Jr. Morphometric demonstration of atrophic changes in the cerebral cortex, white matter, and neostriatum in Huntington's disease. J Neuropathol Exp Neurol 1988;47(5):516-525.
30. Deidda G, Parrini M, Naskar S, Bozarth IF, Contestabile A, Cancedda L. Reversing excitatory GABAAR signaling restores synaptic plasticity and memory in a mouse model of Down syndrome. Nat Med 2015;21(4):318-326.
31. Jiang R, Diaz-Castro B, Looger LL, Khakh BS. Dysfunctional calcium and glutamate signaling in striatal astrocytes from Huntington's disease model mice. J Neurosci 2016;36(12):3453-3470.
32. Becanovic K, Norremolle A, Neal SJ, et al. A SNP in the HTT promoter alters NF-kappaB binding and is a bidirectional genetic modifier of Huntington disease. Nat Neurosci 2015;18(6):807-816.
33. Steed PM, Tansey MG, Zalevsky J, et al. Inactivation of TNF signaling by rationally designed dominant-negative TNF variants. Science 2003;301(5641):1895-1898.
34. Flemmer AW, Gimenez I, Dowd BF, Darman RB, Forbush B. Activation of the Na-K-Cl cotransporter NKCC1 detected with a phospho-specific antibody. J Biol Chem 2002;277(40):37551-37558.
35. Wheelock VL, Tempkin T, Marder K, et al. Predictors of nursing home placement in Huntington disease. Neurology 2003;60(6):998-1001.
36. Ross CA, Pantelyat A, Kogan J, Brandt J. Determinants of functional disability in Huntington's disease: role of cognitive and motor dysfunction. Mov Disord 2014;29(11):1351-1358.
37. Huntington Study G. Tetrabenazine as antichorea therapy in Huntington disease: a randomized controlled trial. Neurology 2006;66 (3):366-372.
38. Dargaei Z, Bang JY, Mahadevan V, et al. Restoring GABAergic inhibition rescues memory deficits in a Huntington's disease mouse model. Proc Natl Acad Sci U S A 2018;115(7):E1618-E1626.
39. Cepeda-Prado E, Popp S, Khan U, et al. R6/2 Huntington's disease mice develop early and progressive abnormal brain metabolism and seizures. J Neurosci 2012;32(19):6456-6467.
40. Dzhala VI, Kuchibhotla KV, Glykys JC, et al. Progressive NKCC1-dependent neuronal chloride accumulation during neonatal seizures. J Neurosci 2010;30(35):11745-11761.
41. Palma E, Amici M, Sobrero F, et al. Anomalous levels of Cl- transporters in the hippocampal subiculum from temporal lobe epilepsy patients make GABA excitatory. Proc Natl Acad Sci U S A 2006; 103(22):8465-8468.
42. Topper JN, Wasserman SM, Anderson KR, Cai J, Falb D, Gimbrone MA Jr. Expression of the bumetanide-sensitive Na-K-Cl cotransporter BSC2 is differentially regulated by fluid mechanical and inflammatory cytokine stimuli in vascular endothelium. J Clin Invest 1997;99(12):2941-2949.
43. Nguyen M, Pace AJ, Koller BH. Mice lacking NKCC1 are protected from development of bacteremia and hypothermic sepsis secondary to bacterial pneumonia. J Exp Med 2007;204(6):1383-1393.
44. Prestridge DS. Predicting Pol II promoter sequences using transcription factor binding sites. J Mol Biol 1995;249(5):923-932.
45. Messeguer X, Escudero R, Farre D, Nunez O, Martinez J, Alba MM. PROMO: detection of known transcription regulatory elements using species-tailored searches. Bioinformatics 2002;18(2):333-334.
46. Jayakumar AR, Tong XY, Ruiz-Cordero R, et al. Activation of NF-kappaB mediates astrocyte swelling and brain edema in traumatic brain injury. J Neurotrauma 2014;31(14):1249-1257.
47. Zhang M, Cui Z, Cui H, Wang Y, Zhong C. Astaxanthin protects astrocytes against trauma-induced apoptosis through inhibition of NKCC1 expression via the NF-kappaB signaling pathway. BMC Neurosci 2017;18(1):42.
48. Khoshnan A, Ko J, Watkin EE, Paige LA, Reinhart PH, Patterson PH. Activation of the IkappaB kinase complex and

nuclear factor-kappaB contributes to mutant huntingtin neurotoxicity. J Neurosci 2004;24(37):7999-8008.

49. Crotti A, Benner C, Kerman BE, et al. Mutant Huntingtin promotes autonomous microglia activation via myeloid lineage-determining factors. Nat Neurosci 2014;17(4):513-521.
50. Wilson CJ, Kawaguchi Y. The origins of two-state spontaneous membrane potential fluctuations of neostriatal spiny neurons. J Neurosci 1996;16(7):2397-2410.
51. Stern EA, Jaeger D, Wilson CJ. Membrane potential synchrony of simultaneously recorded striatal spiny neurons in vivo. Nature 1998;394(6692):475-478.
52. Fino E, Glowinski J, Venance L. Effects of acute dopamine depletion on the electrophysiological properties of striatal neurons. Neurosci Res 2007;58(3):305-316.
53. Dehorter N, Guigoni C, Lopez C, et al. Dopamine-deprived striatal GABAergic interneurons burst and generate repetitive gigantic IPSCs in medium spiny neurons. J Neurosci 2009;29(24):7776-7787.
54. Gittis AH, Kreitzer AC. Striatal microcircuitry and movement disorders. Trends Neurosci 2012;35(9):557-564.
55. Dzhala V, Valeeva G, Glykys J, Khazipov R, Staley K. Traumatic alterations in GABA signaling disrupt hippocampal network activity in the developing brain. J Neurosci 2012;32(12):4017-4031.
56. Shulga A, Magalhaes AC, Autio H, et al. The loop diuretic bumetanide blocks posttraumatic p75NTR upregulation and rescues injured neurons. J Neurosci 2012;32(5):1757-1770.
57. Plotkin JL, Day M, Peterson JD, et al. Impaired TrkB receptor signaling underlies corticostriatal dysfunction in Huntington's disease. Neuron 2014;83(1):178-188.
58. Chen X, Kintner DB, Baba A, Matsuda T, Shull GE, Sun D. Protein aggregation in neurons following OGD: a role for Na+ and Ca2+ ionic dysregulation. J Neurochem 2010;112(1):173-182.
59. Beck J, Lenart B, Kintner DB, Sun D. Na-K-Cl cotransporter contributes to glutamate-mediated excitotoxicity. J Neurosci 2003;23(12):5061-5068.
60. Wang J, Wang CE, Orr A, Tydlacka S, Li SH, Li XJ. Impaired ubiquitin-proteasome system activity in the synapses of Huntington's disease mice. J Cell Biol 2008;180(6):1177-1189.
61. Shekarabi M, Zhang J, Khanna AR, Ellison DH, Delpire E, Kahle KT. WNK Kinase signaling in ion homeostasis and human disease. Cell Metab 2017;25(2):285-299.
62. Zhou Y, Sun W, Chen N, et al. Discovery of NKCC1 as a potential therapeutic target to inhibit hepatocellular carcinoma cell growth and metastasis. Oncotarget 2017;8(39):66328-66342.
63. Modol L, Santos D, Cobianchi S, Gonzalez-Perez F, Lopez-Alvarez V, Navarro X. NKCC1 activation is required for myelinated sensory neurons regeneration through JNK-dependent pathway. J Neurosci 2015;35(19):7414-7427.
64. Ben-Ari Y. NKCC1 chloride importer antagonists attenuate many neurological and psychiatric disorders. Trends Neurosci 2017;40(9):536-554.
65. Rahmanzadeh R, Eftekhari S, Shahbazi A, et al. Effect of bumetanide, a selective NKCC1 inhibitor, on hallucinations of schizophrenic patients; a double-blind randomized clinical trial. Schizophr Res 2017;184:145-146.
66. Lemonnier E, Villeneuve N, Sonie S, et al. Effects of bumetanide on neurobehavioral function in children and adolescents with autism spectrum disorders. Transl Psychiatry 2017;7(5):e1124.
67. Damier P, Hammond C, Ben-Ari Y. Bumetanide to treat Parkinson disease: a report of 4 cases. Clin Neuropharmacol 2016;39(1):57-59.
68. Eftekhari S, Mehvari Habibabadi J, Najafi Ziarani M, et al. Bumetanide reduces seizure frequency in patients with temporal lobe epilepsy. Epilepsia 2013;54(1):e9-e12.

Supporting Data

Additional Supporting Information may be found in the online version of this article at the publisher's web-site.